AD/A-000 582

THE ELLIPTICITY FILTER-A PROPOSED SOLUTION TO THE MIXED EVENT PROBLEM IN NUCLEAR SEISMIC DISCRIMINATION

Eric Posmentier, et al

Ocean and Atmospheric Science, Incorporated

Prepared for:

Air Force Office of Scientific Research
Advanced Research Projects Agency

7 September 1974

DISTRIBUTED BY:

NTIS
National Technical Information Service
U. S. DEPARTMENT OF COMMERCE

UNCLASSIFIED

SECURITY CLASSIFICATION OF THIS PAGE (When Data Entered)

REPORT DOCUMENTATION PAGE		READ INSTRUCTIONS BEFORE COMPLETING FORM
1. REPORT NUMBER AFOSR - TR - 74 - 1640	2. GOVT ACCESSION NO.	3. RECIPIENT'S CATALOG NUMBER AD/A-000 582
4. TITLE (and Subtitle) THE ELLIPTICITY FILTER-A PROPOSED SOLUTION TO THE MIXED EVENT PROBLEM IN NUCLEAR SEISMIC DISCRIMINATION		5. TYPE OF REPORT & PERIOD COVERED Quarterly: April 1, 1974 to June 30, 1974
		6. PERFORMING ORG. REPORT NUMBER TR 74-232
7. AUTHOR(s) Eric Posmentier, Russell Gershman, Bernard Harris		8. CONTRACT OR GRANT NUMBER(s) F44620-74-C-0066
9. PERFORMING ORGANIZATION NAME AND ADDRESS Ocean & Atmospheric Science, Inc. 145 Palisade Street, Dobbs Ferry, NY 10522		10. PROGRAM ELEMENT, PROJECT, TASK AREA & WORK UNIT NUMBERS 62701E AO 1827
11. CONTROLLING OFFICE NAME AND ADDRESS Advanced Research Projects Agency/NMR 1400 Wilson Boulevard, Arlington, VA 22209		12. REPORT DATE Sept 7, 1974
		13. NUMBER OF PAGES 41
14. MONITORING AGENCY NAME & ADDRESS(if different from Controlling Office) Air Force Office of Scientific Research/NP 1400 Wilson Boulevard Arlongton, VA 22209		15. SECURITY CLASS. (of this report) UNCLASSIFIED
		15a. DECLASSIFICATION DOWNGRADING SCHEDULE

16. DISTRIBUTION STATEMENT (of this Report)

Approved for public release; distribution unlimited

17. DISTRIBUTION STATEMENT (of the abstract entered in Block 20, if different from Report)

18. SUPPLEMENTARY NOTES

Nuclear seismic discrimination; surface wave; ellipticity constraint; mixed events.

19. KEY WORDS (Continue on reverse side if necessary and identify by block number)

Nuclear seismic discrimination; surface waves; ellipticity constraint; mixed events;

20. ABSTRACT (Continue on reverse side if necessary and identify by block number)

A proposed solution to the mixed event problem in nuclear seismic discrimination, termed the "ellipticity filter," is cast in the form of a solution of the superposition equations defining the signals from a three-component seismometer station.

Two cases of superposed signals are considered: Rayleigh with Rayleigh; Rayleigh with Love. Using the ellipticity constraint at the seismometer

(over)

DD FORM 1 JAN 73 1473 EDITION OF 1 NOV 65 IS OBSOLETE

UNCLASSIFIED

SECURITY CLASSIFICATION OF THIS PAGE (When Data Entered)

20. Abstract (continued)

station site, the superposition equations defining each case are solved in closed form to yield the unknown complex source amplitudes and source azimuths.
Actual filter procedure involves dividing the component signals into time intervals, taking the Fourier Transform for each time interval, and operating on each of the frequency components in a time interval with the ellipticity filter. The source waveforms are recreated by an inverse transform of those complex amplitudes associated with the same azimuth.
Preliminary evaluation of this technique has been performed and in the noiseless case, has perfectly separated two mixed Rayleigh waves.

OAS

OCEAN & ATMOSPHERIC SCIENCE, INC.
145 PALISADE STREET
DOBBS FERRY, NEW YORK 10522
914-693-9001

TR 74-232

THE ELLIPTICITY FILTER
A PROPOSED SOLUTION
TO THE MIXED EVENT PROBLEM
IN NUCLEAR SEISMIC DISCRIMINATION

by

Eric Posmentier

Russell Gershman

Bernard Harris

Submitted under Contract No. F44620-74-C-0066

Prepared for:

Air Force Office of Scientific Research
1400 Wilson Boulevard
Arlington, Virginia 22209

September 7, 1974

Form Approved
Budget Bureau No. 22-R0293

OAS

OCEAN & ATMOSPHERIC SCIENCE, INC.
145 PALISADE STREET
DOBBS FERRY, NEW YORK 10522
914-693-9001

QUARTERLY TECHNICAL REPORT NO. 1

For Period April 1, 1974 to June 30, 1974

Sponsored by
Advanced Research Projects Agency
ARPA Order No. 1827

ARPA Order Number:	1827
Program Code Number:	4F10
Name of Contractor:	Ocean & Atmospheric Science, Inc.
Effective Date of Contract:	April 1, 1974
Contract Expiration Date:	March 31, 1975
Amount of Contract Dollars:	$128,579
Contract Number:	F44620-74-C-0066
Principal Investigator and Phone Number:	Dr. Bernard Harris 914-693-9001
Program Manager and Phone Number:	Russell Gershman 914-693-9001
Short Title of Work:	Seismic Verification of Mixed Events

This research was supported by the Advanced Research Projects Agency of the Department of Defense and was monitored by the Air Force Office of Scientific Research under Contract No. F44620-74-C-0066

TABLE OF CONTENTS

1.0 Introduction and Summary

One of the important aspects of any underground nuclear test ban treaty is the ability to verify that the signators are adhering to the agreed provisions. To this end, reliable methods for detecting underground nuclear events must be employed. A method which has proven to be quite useful in this application has been seismic verification.

Seismic verification of a test ban on underground nuclear explosions requires the classification of seismic events at teleseismic (large) distances. Classification is determined by examining properties of the seismic waves as recorded at seismometer stations located around the world. Two wave types are important in the classification process. These are body waves, travelling through the earth, and surface waves, travelling along the earth's surface. Since both earthquakes and nuclear explosions generate short-period body waves and long-period surface waves, the conventional criteria used to distinguish between earthquake and explosion sources, such as the widely used surface-to-body magnitude ratio ($M_s : m_b$) criterion, depend on freeing these surface and body waves as much as possible from interfering noise and other waves from overlapping events.

The detection threshold for events has been reduced to body magnitudes (m_b) on the order of 4.0 by the advent of large aperture arrays such as LASA, NORSAR and ALPA. Similarly, the development

of very-low period high-gain seismometers promises similar reductions for detecting surface waves and estimating their magnitude.

One of the major problems still remaining, is estimating the surface wave magnitude (M_s) of an event when overlapping or mixed events are present. Since mixed events are often a natural occurrence for multiple earthquakes, underground testing evasion tactics might include timing the test to coincide with a local earthquake or with the coda of a large earthquake. According to the Conference of the Committee of Disarmament, on the average, about 16 percent of the total possible single station observations were mixed events, in which interfering signals from an overlapping event made it impossible to extract reliable amplitude or spectral information from the wave form.

The mixed event problem can be more clearly defined as separating the Rayleigh or Love primary surface waves of a desired event from a waveform which is the sum of the desired event and:

1. a Rayleigh or Love (or both) primary surface wave of an interfering event,
2. the coda of a large earthquake.

Due to the high signal-to-noise ratio made possible by the VLP high gain seismometers, OAS proposed to investigate signal processing methods which were capable of discrimination of mixed events in a low noise environment. Among these methods were included:

1. Polarization Filter

2. Azimuthal Filter

3. Homomorphic Decompostion/Complex Cepstrum

4. Complex Demodulation

5. Matched Filters

6. Large Array Processing

In addition to these, two other techniques by Alexander concerning separation of Love waves from Rayleigh wave interference were found.

As an extension to the methods of Alexander and the concepts of the polarization and azimuthal filters, OAS has developed a filter termed the "ellipticity" filter which has the capability of separating two superposed Rayleigh waves or one Rayleigh and one Love wave. Briefly, the ellipticity filter processes the three signal outputs of a three component seismometer station using the value of ellipticity at the station to produce the complex amplitudes and azimuths of the two superposed surface waves.

The record is divided into a number of intervals, the interval length being determined by the time variability of the interfering wave. For each interval, the waveform is transformed into the frequency domain. Each frequency bin is now defined by three complex numbers, one each for the vertical and the two horizontal channels.

Using the value of ellipticity of the station site, the superposition equations for the case of two Rayleigh waves or one Rayleigh and one Love wave may be written for each frequency bin. These equations have been solved in closed form giving the two complex source amplitudes and their respective azimuths in terms of the three complex data points and the ellipticity.

Having solved the equations for all frequency bins, the inverse transform of those complex amplitudes associated with one source azimuth value yields the surface waveform for that source. Similarly, the inverse transform of the complex amplitudes associated with the other source azimuth yields the second surface waveform.

Similarly derived waveforms for other time intervals in the record may be combined smoothly to yield the overall surface waveforms.

The main limitations in this method are those imposed by the additions of ambient noise to the superposed surface waves. The superposition equations have been solved in a deterministic manner and additive noise will clearly alter the accuracy of the results. In addition, the noise sensitivity of the solution may be greater for small azimuthal source separations than for large separation. These and other aspects concerning additive noise are being investigated .

to yield limitations of this approach. This investigation includes both theoretical studies and empirical studies and simulations.

In addition, the method is based on the fact that the ellipticity remains constant for all azimuth around the station site. Nothing in the literature has been found to prove or disapprove this assumption for the VLP waves in question. Thus, we are initiating an effort to determine whether or not ellipticity exhibits azimuthal dependence at a given site by calculating the ellipticity for a number of earthquakes of differing azimuths at the site.

Section 2 of this report reviews the methods investigated to date, namely the polarization and azimuthal filters and the two methods by Alexander. The other signal processing methods listed are being looked into. Section 3 formulates the problem mathematically and gives the solution method comprising the ellipticity filter approach. Section 4 describes some preliminary computer simulation testing of the filter while Section 5 outlines areas for future investigation and testing of the filter.

to yield limitations of this approach. This investigation includes both theoretical studies and empirical studies and simulations.

In addition, the method is based on the fact that the ellipticity remains constant for all azimuth around the station site. Nothing in the literature has been found to prove or disapprove this assumption for the VLP waves in question. Thus, we are initiating an effort to determine whether or not ellipticity exhibits azimuthal dependence at a given site by calculating the ellipticity for a number of earthquakes of differing azimuths at the site.

Section 2 of this report reviews the methods investigated to date, namely the polarization and azimuthal filters and the two methods by Alexander. The other signal processing methods listed are being looked into. Section 3 formulates the problem mathematically and gives the solution method comprising the ellipticity filter approach. Section 4 describes some preliminary computer simulation testing of the filter while Section 5 outlines areas for future investigation and testing of the filter.

2.0 Review of Existing Techniques

The ellipticity filter concept is an extension of the azimuthal and polarization filter techniques of Choy and McCamy[4] as well as waveform separation algorithms presented by Alexander. These techniques, in addition to others, are reviewed in the following section with emphasis being placed on their utilization in the mixed event problem.

2.1 The Polarization Filter

The polarization filter, as developed by Choy and McCamy, was designed to separate a 90° polarized Rayleigh wave from interfering waves by retaining information in those time-frequency bins which possess the desired attribute of a 90° phase shift between the vertical and horizontal components of a three component seismometer. This filter, thus, utilizes those advantageous moments in which the interference is small compared to the signal.

For a given time interval, the filter computes the Fourier transform of the vertical and one of the horizontal components of a three-component seismometer. For each frequency component in the desired passband, the polarization filter generates a filter function proportional to the phase difference between the vertical and the selected horizontal component. The filter function used by Choy and

McCamy is

$$F(\omega) = \sin^N[\phi_Z(\omega) - \phi_X(\omega)]$$

where $\phi_Z(\omega)$ and $\phi_X(\omega)$ are the phases of the vertical and selected horizontal components respectively and N is a constant which determines the fall-off. The filtered output is calculated by multiplying the Fourier transform of the signal by $F(\omega)$. Thus, a component having a phase difference near 90^o, as for a pure Rayleigh wave, will be passed, whereas non-Rayleigh type signals will be rejected.

The inverse transform of the filtered components is taken to yield a time waveform for the interval. This procedure is repeated for a number of overlapping time intervals required for the entire signal. The resultant filtered waveforms are added using a smoothing algorithm to yield a continuous time function.

The main disadvantage of this approach seems to be that, even a small amount of interference in a given time-frequency bin may sufficiently corrupt the waveform so that it is partially rejected. If two Rayleigh waves are superposed, the filter will either attenuate or pass the mixed signal depending on the phase difference of the mixed signal. In either case, the desired event has not been separated. In the Rayleigh:Love mixed event, the Rayleigh wave will pass only if it significantly dominates the Love wave. If the Love wave dominates, then the record will be attenuated.

2.2 The Azimuthal Filter

The azimuthal filter, also developed by Choy and McCamy, was intended to separate a Love wave from interfering waves by retaining information in those time-frequency bins in which the azimuth, calculated from the two horizontal components, is near to an a priori azimuth value.

The same procedure is followed as for the polarization filter except that the two horizontal components are processed. A filter function $F(\omega)$ is generated by the filter and has the form

$$F(\omega) = \sin^N \left[\alpha - \tan^{-1} \frac{Y(\omega)}{X(\omega)} \right]$$

Thus, if the azimuth of the signal component is near that expected, the component is passed. If not, the component is attenuated.

The azimuthal filter is intended to separate Love waves from Rayleigh by passing the Love wave when it dominates the signal. However, even the presence of a smaller interfering signal can perturbate the azimuth, thus attenuating the record. For instance, the particle motion of a Rayleigh wave from the same azimuth as the Love wave is orthogonal to the particle motion of the Love wave. Thus, if the Rayleigh wave has an amplitude of -6dB with respect to the Love wave, the apparent azimuth of the combined wave is 27° from the

actual azimuth value for the Love wave. A coefficient of N=8 in the filter function, $F(\omega)$, causes a 5dB attenuation of this component.

2.3 Frequency Dependent Rotation of Axis

A method suggested by Alexander would separate Love waves from interfering Rayleigh waves by a frequency dependent rotation of the horizontal axis. This method requires the previously determined azimuth of arrival of the Rayleigh interference on a frequency dependent basis. The azimuthal dependence on frequency is based on the lateral refraction of Rayleigh waves off ocean-continent boundaries being frequency dependent. Using this azimuth information, a node is placed in the direction of the azimuth of arrival on a per frequency basis by a suitable rotation of horizontal coordinates. This node eliminates the Rayleigh components leaving only the desired Love components (assuming that the azimuth of arrival of the Love wave is not 90^{o} from the Rayleigh).

This method would clearly be applicable to the mixed event in which two Rayleigh waves are superposed, assuming their azimuths are not identical. The only disadvantage lies in determining the azimuth of arrival of the event to be eliminated. Alexander suggests that an array using F-k processing would be a likely method.

2.4 Frequency Dependent Subtraction of Rayleigh Interference using the Ellipticity Constraint

A second method proposed by Alexander for separating Love waves from Rayleigh interference is to subtract out the Rayleigh components in the horizontal signals using the azimuth of arrival of the Rayleigh signal and the ellipticity constraint between the vertical and horizontal components of a Rayleigh wave. Since the vertical component contains only the Rayleigh interference, the azimuth of arrival and the ellipticity constraint define the amount of Rayleigh interference contained in each horizontal component. When the interfering components are subtracted, the resulting signal should be the desired Love components. This procedure would also be done on a per frequency basis since the azimuth of arrival of the Rayleigh interference may be frequency dependent.

As in the previous method, the azimuth of the interfering Rayleigh wave must be accurately determined to yield successful results. In addition, the ellipticity constraint at the station site must be learned in order to subtract out the correct amount of interference.

Utilizing this method for the Rayleigh:Rayleigh mixed event problem implies determination of the complex amplitude and the azimuth of the interfering Rayleigh wave since the vertical signal now contains components of both signals.

3.0 The Seismic Ellipticity Filter

In an effort to utilize the information represented by a three-component seismometer station, a decomposition algorithm termed the "Seismic Ellipticity Filter" has been developed. As input, this filter accepts the superposition of two independent surface waves (either Rayleigh or one Rayleigh and one Love) from different azimuths. Using the ellipticity constraint defining the radial-to vertical amplitude ratio of a Rayleigh wave, the ellipticity filter operates on this input and, in the noiseless case, perfectly separates the superposed signals into the two original waveforms. In addition, the azimuths of the two waves are determined.

In general, the filter operation is valid for high signal-to-noise ratios and initially solutions are found only for the noise-free case.

This filter is an outgrowth of the azimuthal and polarization filter concepts of Choy and McCamy and an extension of the method of Alexander, discussed in Section 2.4, to utilize the ellipticity constraint in separating Love waves from Rayleigh interference. In our case, the ellipticity constraint is used to formulate the superposition equations defining the three seismometer signals. This formulation allows us to solve both the Rayleigh wave with superposed Rayleigh wave interference problem as well as the Love wave with superposed

Rayleigh wave interference problem.

The desired wave can either be the Love or Rayleigh, while the interfering wave is generally considered Rayleigh. The most frequent problem is that of an event being masked by earthquake coda which is considered to be Rayleigh in character. In the following development, the two waves will be designated simply by Source 1 and Source 2, since the filter solves for both waves and does not care which is signal and which is interference.

3.1 Problem Statement

> Given the outputs of three seismometer components (E/W, N/S, and vertical), devise a method which can extract a desired primary surface wave, either Rayleigh or Love, from signals which are the superposition of the desired wave, with an interfering Rayleigh surface wave.

Since the filter operates in the frequency domain, the three seismometer components, E/W, N/S, and vertical, are represented by their Fourier Transforms as X, Y, and Z respectively, and X denotes the j^{th} frequency component of X.

The following assumptions concerning signal and filter parameters are made:

1. Only two unknown signals are present in any specific time interval of observables being processed. These signals must either be both Rayleigh or one Rayleigh and one Love.

The superposition equations which define the observable quantities are limited by the number of independent seismometer components, in this case, three. Each of the observables, X_j, Y_j,

and Z_j is a complex quantity and, therefore, represents two real superposition equations. Altogether, there are six real superposition equations which define the three complex observables.

Each unknown signal represents three real unknowns: an amplitude, phase and azimuth. Thus, two unknown signals represent six real unknowns, the same number as the number of real superposition equations. Hence, more than two unknown signals could not be solved by using only three independent seismometer components. Similarly, two Love waves cannot be solved as the problem contains six unknowns but only four real equations, since the vertical component contains no information.

Due to the dispersive nature of seismic surface wave signals, for a time interval small compared to the primary surface wave duration, most of the energy of the surface wave in that interval will be concentrated in a few spectral components. Thus, a third unknown signal may possibly be resolved if it is significantly shifted in time such that its contribution to the major frequency components for the two unknown signals is negligible.

2. The observables are noise-free.

The superposition equations defining the ellipticity filter do not contain explicit noise terms but are a set of six deterministic equations in six unknowns. Clearly the closed form solutions will be degraded in the presence of noise. It is felt, though, that a high signal-to-

noise ratio environment will still yield satisfactory results. The threshold for such operations has yet to be determined.

3. The apparent ellipticity at the seismometer station site is known and does not vary with azimuth of arrival.

The apparent ellipticity is a complex quantity which equals the radial component divided by the vertical component of a pure Rayleigh wave, where these quantities are measured at the output of the seismometers. Thus, any seismometer phase shift or amplitude scale factor is included in this factor.

3.2 Seismic Filter Configuration

The seismic filter conifguration is shown in Figure 3.1. This pictorial representation shows the method followed for the k^{th} time interval.

The three seismometer component waveforms, x(t), y(t), and z(t), are sampled in time to yield $x_i(t)$, $y_i(t)$, and $z_i(t)$. These waveforms are divided into either adjacent or overlapping time intervals, the k^{th} interval denoted by a superscript k. The duration of this time interval depends mainly on the time variability expected in the azimuth of arrival. For coda-type interference, the consensus[3,4] appears to be intervals of approximately 2-3 minutes.

For the time intervals selected, the Fast Fourier Transforms of x_i, y_i, and z_i are taken to yield X_j^k, Y_j^k, and Z_j^k, where X_j^k

denotes the j^{th} frequency component in the k^{th} time interval of x(t).

For each frequency component in each time interval, solve the superposition equations (see Sections 3.3 and 3.4) for the two unknown complex amplitudes A_{1j}^{k} and A_{2j}^{k} and their respective azimuths θ_1^{k} and θ_2^{k}.

In the k^{th} interval associated with Source 1, are those complex amplitudes having azimuth θ_1^{k}. Associate with Source 2 all those complex amplitudes having azimuth θ_2^{k}. Take the inverse Fourier Transform of those complex amplitudes associated with Source 1, yielding the signal $a_1^{k}(t)$. Similarly, take the inverse Transform of all those complex amplitudes associated with Source 2, yielding $a_2^{k}(t)$.

Over all k of interest, smooth those resultant time waveforms associated with Source 1 in which θ_1^{k} is the same. The resultant waveform is the total waveform for Source 1. Repeat for Source 2.

3.3 The Seismic Ellipticity Filter for Rayleigh: Rayleigh Mixed Events

Based on the source geometry given in Figure 3.2, the superposition equations defining the observables X_j^{k}, Y_j^{k}, and Z_j^{k} for two Rayleigh sources are given by

$$X_j^k = -f(A_{1j}^k \sin \theta_1 + A_{2j}^k \sin \theta_2)$$

$$Y_j^k = -f(A_{1j}^k \cos\theta_1 + A_{2j}^k \cos\theta_2)$$

$$Z_j^k = A_{1j}^k + A_{2j}^k$$

where f is the apparent ellipticity at the station site.

These three complex equations actually represent six equations by separating real and imaginary parts. There are six unknowns: A_{1j}^k and A_{2j}^k are complex and, thus, represent two unknowns each (an amplitude and a phase); the two real azimuths θ_1 and θ_2. Thus, we have six equations with six unknowns. These equations have been solved (See Appendix A) in closed form. For simplicity, we drop the subscripts j and k. The complex amplitudes A_1 and A_2 are given by

$$A_1 = |A_1| e^{i\phi_1}$$

$$A_2 = |A_2| e^{i\phi_2}$$

Thus, the six unknowns A_1, A_2, ϕ_1, ϕ_2, θ_1, and θ_2 are given by

$$|A_1| = \frac{\text{Im}(Z) \cos\phi_2 - \text{Re}(Z) \sin\phi_2}{\sin(\phi_1 - \phi_2)}$$

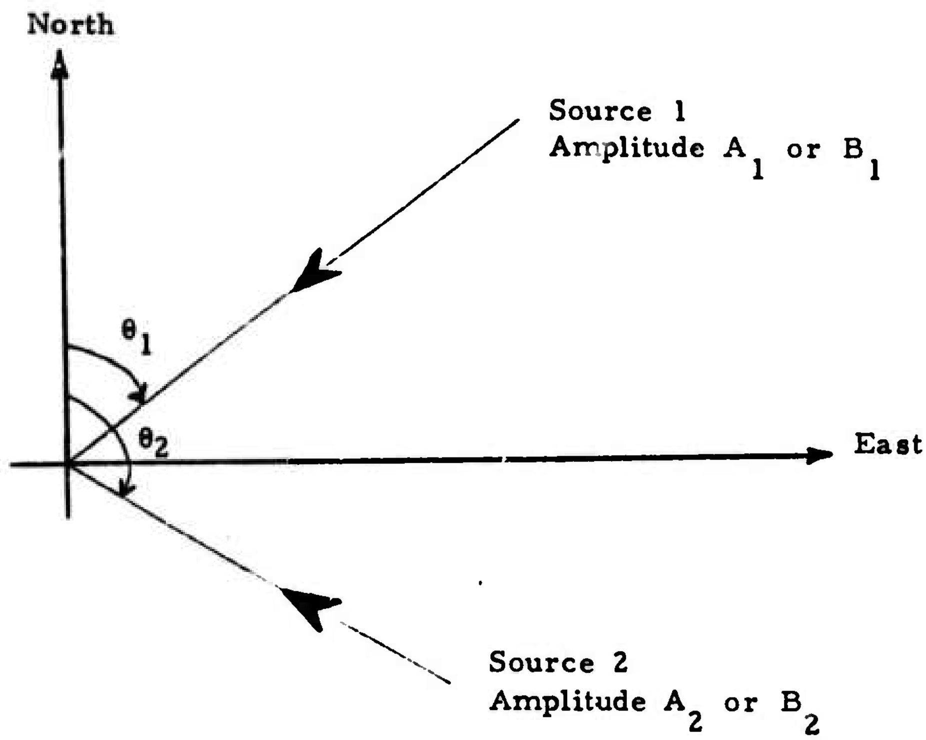

where θ_1, θ_2 are the real azimuths of the two sources,

A_1, A_2 are the complex vertical-component amplitudes for LR (Rayleigh) sources

B_1, B_2 are the total complex horizontal amplitudes for LQ (Love) sources - positive sense to the right of phase velocity.

Fig. 3.2: Source Geometry

$$|A_2| = \frac{\mathrm{Im}(Z)\cos\phi_1 - \mathrm{Re}(Z)\sin\phi_1}{\sin(\phi_2 - \phi_1)}$$

$$\phi_1 = \frac{-b + (b^2 - 4ac)^{1/2}}{2a}$$

$$\phi_2 = \frac{-b - (b^2 - 4ac)^{1/2}}{2a}$$

$$\theta_1 = \arctan \frac{\mathrm{Im}(X) - P_2\,\mathrm{Re}(X)}{\mathrm{Im}(Y) - P_2\,\mathrm{Re}(Y)}$$

$$\theta_2 = \arctan \frac{\mathrm{Im}(X) - P_1\,\mathrm{Re}(X)}{\mathrm{Im}(Y) - P_1\,\mathrm{Re}(Y)}$$

where $P_1 = \arctan\phi_1$, $P_2 = \arctan\phi_2$

$$a = \mathrm{Re}^2\left(\frac{Y}{f}\right) + \mathrm{Re}^2\left(\frac{X}{f}\right) - \mathrm{Re}^2(Z)$$

$$b = 2\left[\mathrm{Re}(Z)\,\mathrm{Im}(Z) - \mathrm{Re}\left(\frac{Y}{f}\right)\mathrm{Im}\left(\frac{Y}{f}\right) - \mathrm{Re}\left(\frac{X}{f}\right)\mathrm{Im}\left(\frac{X}{f}\right)\right]$$

$$c = \mathrm{Im}^2\left(\frac{Y}{f}\right) + \mathrm{Im}^2\left(\frac{X}{f}\right) - \mathrm{Im}^2(Z)$$

Thus, for each frequency band in each time interval, the above set of equations is solved for the two sources and yields the six quantities $|A_1|$, ϕ_1, and θ_1 for source 1 and $|A_2|$, ϕ_2, and θ_2 for source 2. The solutions for all frequency bins in a time interval are

combined by associating with source 1 all those solutions having azimuth θ_1. Similarly, those solutions having azimuth θ_2 are associated with source 2. The time waveform in the k^{th} time interval for source 1 is then calculated by summing those sinusoids associated with source 1. Thus,

$$s_1^k(t) = \sum_j |A_{1j}^k| \sin(\omega_j t + \phi_{1j}^k)$$

Similarly,

$$s_2^k(t) = \sum_j |A_{2j}^k| \sin(\omega_j t + \phi_{2j}^k)$$

This procedure is applied over all time intervals defining the record. The overall signals $s_1(t)$, [or $s_2(t)$], are then formed by summing in some smooth manner the interval waveforms $s_1^k(t)$ over k.

3.4 The Seismic Ellipticity Filter for Raleigh: Love Mixed Events

For the Love:Rayleigh mixed event, the superposition equations defining the observables X_j^k, Y_j^k, and Z_j^k are given by

$$X_j^k = -f A_{1j}^k \sin\theta_1 - B_{2j}^k \cos \theta_2$$

$$Y_j^k = -f A_{1j}^k \cos \theta_1 + B_{2j}^k \sin \theta_2$$

$$Z_j^k = A_{1j}^k$$

where f is the apparent ellipticity and B_2 represents the complex amplitude of the Love wave.

As in Appendix B, these three complex equations represent six real equations in the six unknowns Re A_1, Im A_1, Re B_2, Im B_2, θ_1 and θ_2:

$$\theta_2 = \arctan\left[\frac{\mathrm{Im}(Y) - P\cdot\mathrm{Re}(Y)}{\mathrm{Im}(X) - P\cdot\mathrm{Re}(X)}\right]$$

$$\theta_1 = \theta_2 + \arccos\left[\frac{\mathrm{Re}(\frac{X}{f})\sin\theta_2 + \mathrm{Re}(\frac{Y}{f})\cos\theta_2}{\mathrm{Re}(Z)}\right]$$

$$\mathrm{Im}\,B_2 = \frac{f}{\sin\theta_2}\left[\mathrm{Re}(\frac{Y}{f}) + \mathrm{Re}(Z)\cos\theta_1\right]$$

$$\mathrm{Im}\,B_2 = \frac{f}{\sin\theta_2}\left[\mathrm{Im}(\frac{Y}{f}) + \mathrm{Im}(Z)\cos\theta_1\right]$$

where

$$P = \frac{\mathrm{Im}(Z)}{\mathrm{Re}(Z)}$$

$$\mathrm{Re}A_1 = \mathrm{Re}(Z)$$

$$\mathrm{Im}A_1 = \mathrm{Im}(Z)$$

Combining the solution for all frequency bins and time segments to yield the source waveforms is performed as outlined in Section 3.3

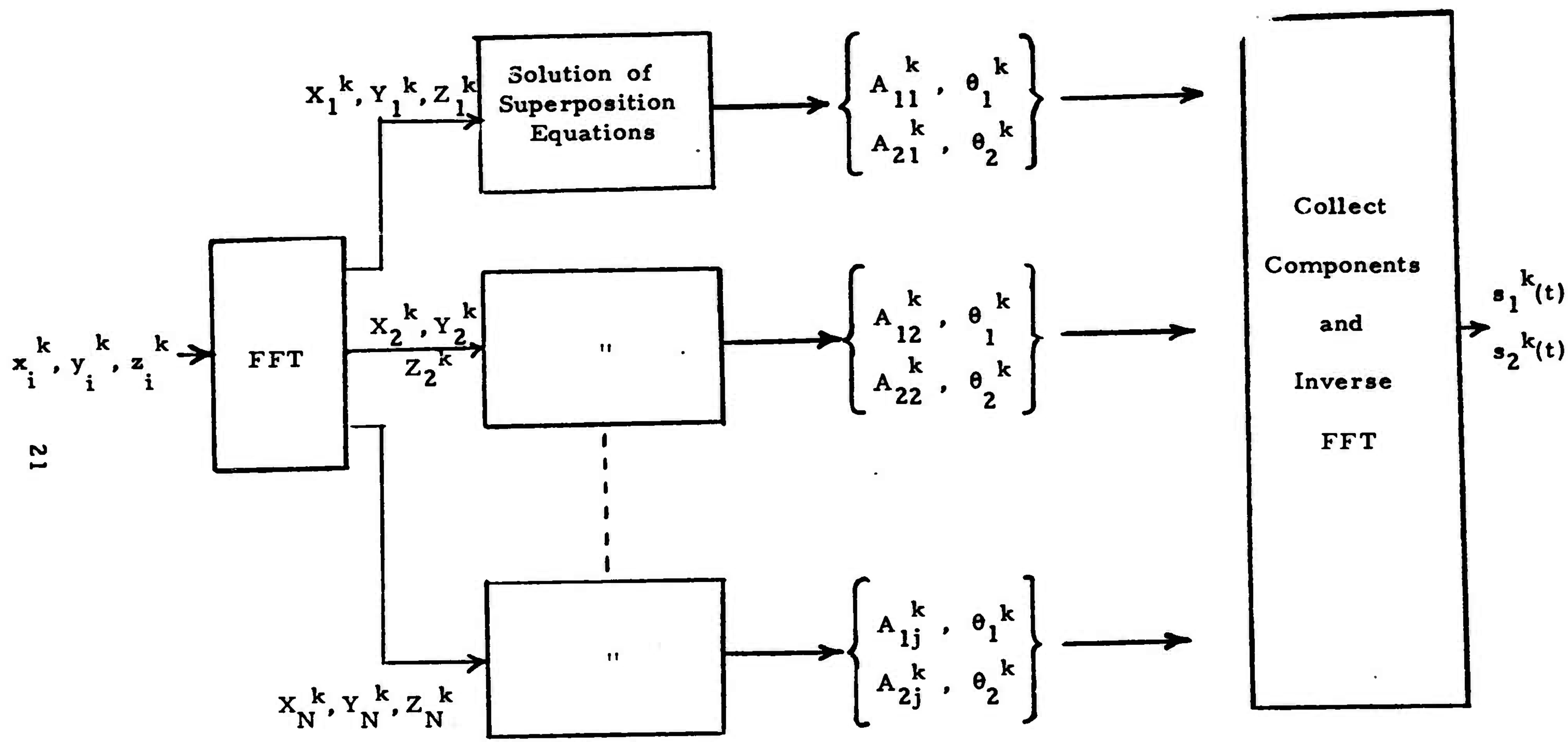

Fig. 3. 1: Block Diagram of Seismic Ellipticity Filter

4.0 Computer Simulation

Some preliminary analysis of the ellipticity filter's operation was performed using simulated input data. A time interval of 180 seconds was chosen. Using that interval, the 3rd through 7th harmonics (29.9 sec, 30.0 sec, 36.0 sec, 45.0 sec, 60.0 sec periods) were used to construct the Airy phase of a Rayleigh waveform. In addition, an interfering coda waveform was similarly constructed. The computer program mixed these two waveforms assuming their propagation paths were orthogonal. The Signal, Coda, and mixed Signal + Coda are shown in Figures 4.1a, b, and c. These are pictures of the vertical component. The horizontal components are not shown. The computer program perfectly separated the mixed Signal + Coda in the Airy signals labeled Output 1 and Output 2, as in Figure 4.1d and e. Note that Output 1 is identical to the input signal while Output 2 is identical to the coda.

The actual computer output is shown in Figure 4.2. This shows seven separate computer runs for seven different signal-to-coda ratio from -9 dB to +9 dB in 3 dB steps. Each run lists the azimuth and the sine and cosine components of the complex amplitude for each of the five frequency bins. The sine and cosine components associated with an azimuth of 0° are the signal while those associated with an azimuth of 90° are the Coda.

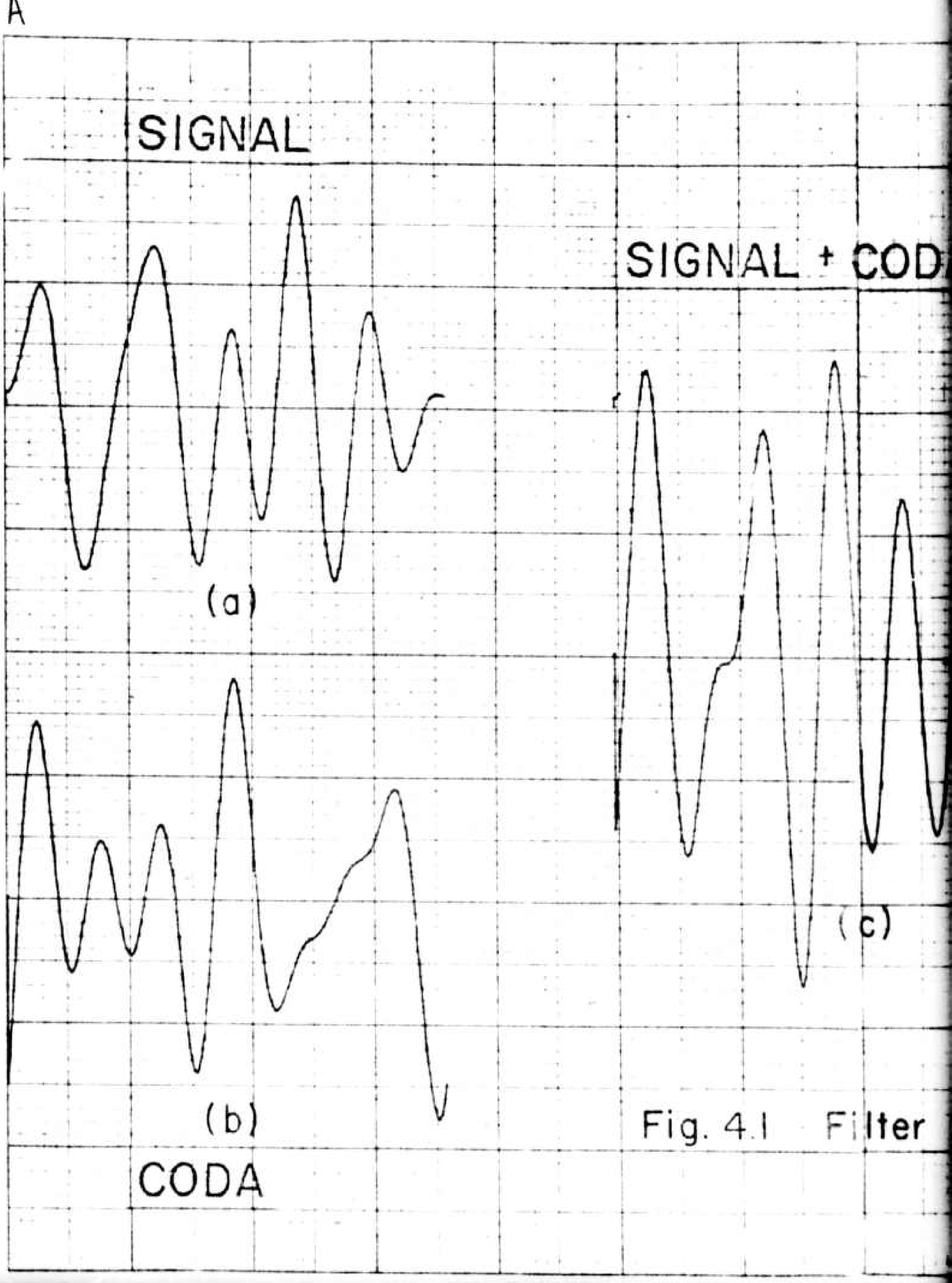

Fig. 4.1 Filter

B

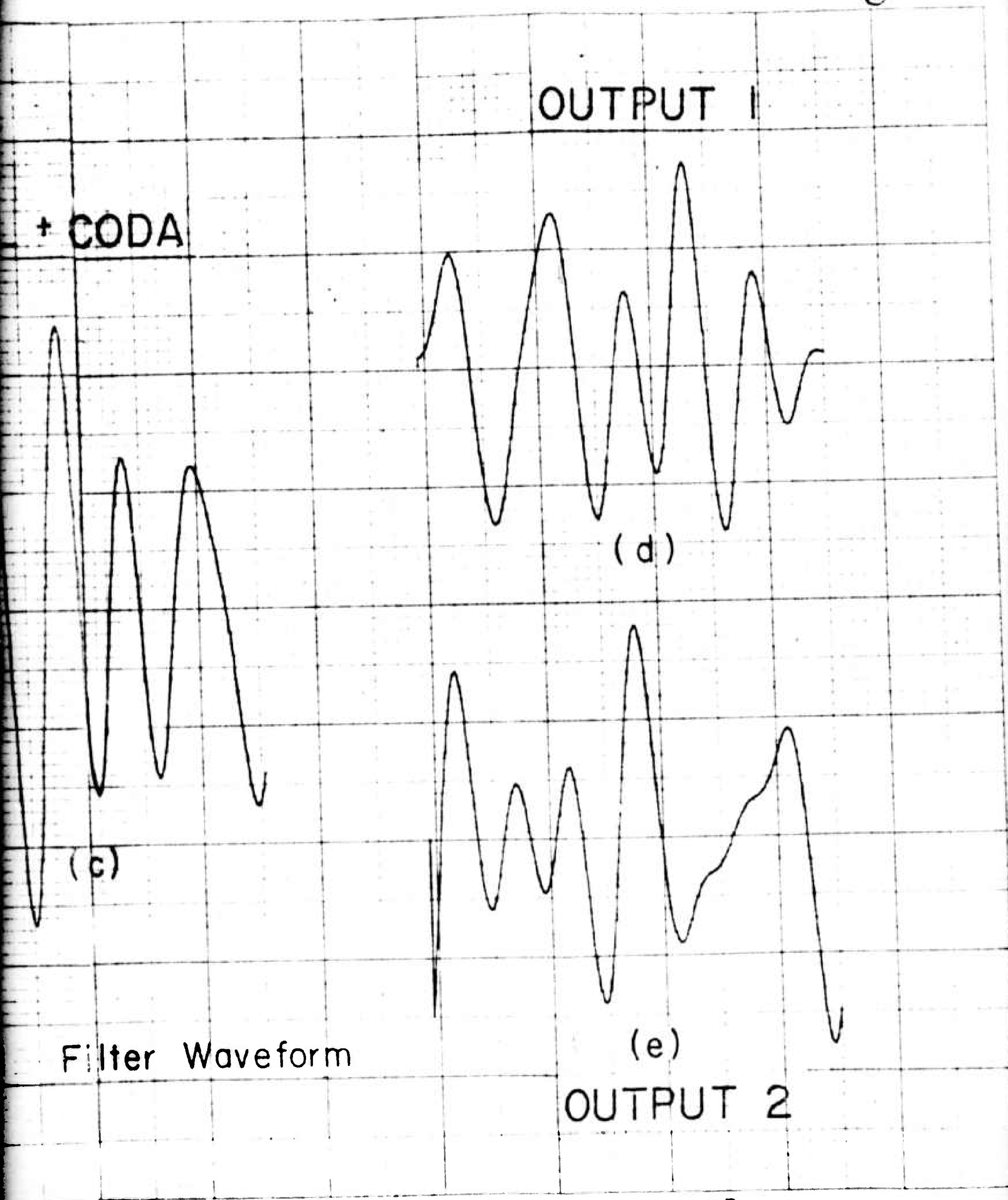

A

XGT.FO

CODA	.3536	PERIOD	60.0 SEC		45.0 SEC		36.0 S
NOISE	.0156	AZIMUTH	90.0	-.00	-.0	90.00	90.0
		SIN COMP	.00	.01	.87	.35	.00
		COS COMP	-.35	1.01	-.50	.00	-.35
CODA	.5000	PERIOD	60.0 SEC		45.0 SEC		36.0 S
NOISE	.0156	AZIMUTH	90.0	-.00	-.0	90.00	90.0
		SIN COMP	.01	.01	.87	.50	.00
		COS COMP	-.49	1.01	-.50	.00	-.50
CODA	.7071	PERIOD	60.0 SEC		45.0 SEC		36.0 S
NOISE	.0156	AZIMUTH	90.0	-.00	.0	90.00	90.0
		SIN COMP	.01	.01	.87	.71	.01
		COS COMP	-.70	1.01	-.50	.01	-.71
CODA	1.0000	PERIOD	60.0 SEC		45.0 SEC		36.0 S
NOISE	.0156	AZIMUTH	90.0	-.00	-.0	90.00	90.0
		SIN COMP	.01	.01	.87	1.00	.01
		COS COMP	-.99	1.01	-.50	.01	-1.00
CODA	1.4142	PERIOD	60.0 SEC		45.0 SEC		36.0 S
NOISE	.0156	AZIMUTH	90.0	-.00	.0	90.00	90.0
		SIN COMP	.01	.01	.87	1.41	.01
		COS COMP	-1.40	1.01	-.50	.01	-1.41
CODA	2.0000	PERIOD	60.0 SEC		45.0 SEC		36.0 S
NOISE	.0156	AZIMUTH	90.0	-.00	-.0	90.00	90.0
		SIN COMP	.02	.01	.87	2.00	.02
		COS COMP	-1.98	1.01	-.50	.02	-2.00
CODA	2.8284	PERIOD	60.0 SEC		45.0 SEC		36.0 S
NOISE	.0156	AZIMUTH	90.0	-.00	-.0	90.00	90.0
		SIN COMP	.03	.01	.87	2.83	.03
		COS COMP	-2.80	1.01	-.50	.03	-2.83

.FIN

Fig. 4.2: Compute

B

45.0 SEC		36.0 SEC		30.0 SEC		25.7 SEC	
-.0	90.00	90.0	.00	90.0	.00	-.0	90.00
.87	.35	.00	.50	.35	.01	-.87	.00
-.50	.00	-.35	-.87	.00	1.00	-.50	-.35
45.0 SEC		36.0 SEC		30.0 SEC		25.7 SEC	
-.0	90.00	90.0	.00	90.0	.00	-.0	90.00
.87	.50	.00	.50	.50	.01	-.87	.00
-.50	.00	-.50	-.87	.00	1.00	-.50	-.50
45.0 SEC		36.0 SEC		30.0 SEC		25.7 SEC	
.0	90.00	90.0	.00	90.0	.00	-.0	90.00
.87	.71	.01	.50	.71	.01	-.87	.01
-.50	.01	-.71	-.87	.01	1.00	-.50	-.71
45.0 SEC		36.0 SEC		30.0 SEC		25.7 SEC	
-.0	90.00	90.0	.00	90.0	.00	-.0	90.00
.87	1.00	.01	.50	1.00	.01	-.87	.01
-.50	.01	-1.00	-.87	.01	1.00	-.50	-1.00
45.0 SEC		36.0 SEC		30.0 SEC		25.7 SEC	
.0	90.00	90.0	.00	90.0	.00	-.0	90.00
.87	1.41	.01	.50	1.41	.01	-.87	.01
-.50	.01	-1.41	-.87	.01	1.00	-.50	-1.41
45.0 SEC		36.0 SEC		30.0 SEC		25.7 SEC	
-.0	90.00	90.0	.00	90.0	.00	-.0	90.00
.87	2.00	.02	.50	2.00	.01	-.87	.02
-.50	.02	-2.00	-.87	.02	1.00	-.50	-2.00
45.0 SEC		36.0 SEC		30.0 SEC		25.7 SEC	
-.0	90.00	90.0	.00	90.0	.00	-.0	90.00
.87	2.83	.03	.50	2.83	.01	-.87	.03
-.50	.03	-2.83	-.87	.03	1.00	-.50	-2.83

Fig. 4.2: Computed Filter Output

5.0 Future Investigation of the Ellipticity Filter

Performance evaluation of the ellipticity filter involves testing in a number of areas. One of the most important is the inclusion of additive noise in the mixed event waveforms to determine the noise level which can be handled before the filter algorithm breaks down. Secondly, the filter may be more susceptible to additive noise when the azimuth of the mixed events are relatively near. Thus, azimuth of the two sources will be a parameter in the noise investigation. A third factor may be the relative strength of the two signals in the presence of additive noise.

Successful filter operation has been based on exact knowledge of the ellipticity. When processing real data, the ellipticity value used may differ from the true value. Thus, we will investigate the effect of variations in the value of ellipticity used on filter operation. In addition, the value of ellipticity at a station site has been assumed independent of the azimuth of arrival. A test will be performed to determine the actual value of ellipticity at a station site and its sensitivity, if any, to the azimuth of arrival.

The above investigations will be performed using both simulated and real VLP high-gain data from the Lamont-Doherty Geological Observatory of Columbia University. Presently, we are compounding a data bank of explosion events, earthquakes, earthquake coda and ambient noise for testing purposes.

APPENDIX A: Derivation of the Ellipticity Filter for Two Mixed Rayleigh Events

Assume we have a three component seismometer with the output signals x(t), y(t), and z(t) being the E/W, N/S and vertical components respectively. Assume that a Fourier Transform of these signals has been taken for some desired time window. The signals X, Y, and Z represent one of the Fourier components for the transformed signals and, thus, are complex functions of frequency.

For the case of two mixed Rayleigh sources, the superposition equations for X, Y, and Z may be written as

$$X = -f (A_1 \sin \theta_1 + A_2 \sin \theta_2) \quad (1)$$

$$Y = -f (A_1 \cos \theta_1 + A_2 \cos \theta_2) \quad (2)$$

$$Z = A_1 + A_2 \quad (3)$$

where A_1 and A_2 are the complex amplitudes of the two Rayleigh events,

θ_1 and θ_2 are the azimuths of A_1 and A_2, respectively,

f is the apparent ellipticity.

The source geometry is given in Figure 3.1, where f is the apparent ellipticity at the receiving site and is assumed known.

From (2)

$$\mathrm{Re} \left(-\frac{Y}{f} \right) = \mathrm{Re} (A_1) \cos \theta_1 + \mathrm{Re} (A_2) \cos \theta_2 \quad (4)$$

$$\mathrm{Im} \left(-\frac{Y}{f} \right) = \mathrm{Im} (A_1) \cos \theta_1 + \mathrm{Im} (A_2) \cos \theta_2 \quad (5)$$

Multiplying (4) by $P_1 \equiv \dfrac{Im(A_1)}{Re(A_1)}$ yields

$$P_1 \cdot Re\left(-\frac{Y}{f}\right) = Im(A_1)\cos\theta_1 + P_1 \cdot Re(A_2)\cos\theta_2 \tag{6}$$

Subtracting (6) from (5)

$$Im\left(-\frac{Y}{f}\right) - P_1 \cdot Re\left(-\frac{Y}{f}\right) = [\,Im(A_2) - P_1 \cdot Re(A_2)\,]\cos\theta_2 \tag{7}$$

Substituting into (7) the value of A_2 from (3),

$$Im\left(-\frac{Y}{f}\right) - P_1 \cdot Re\left(-\frac{Y}{f}\right) = [\,Im(Z) - P_1 \cdot Re(Z)\,]\cos\theta_2 \tag{8}$$

By a similar sequence, equation (1) yields:

$$Im\left(-\frac{X}{f}\right) - P_1 \cdot Re\left(-\frac{X}{f}\right) = [\,Im(Z) - P_1 \cdot Re(Z)\,]\sin\theta_2 \tag{9}$$

Squaring (8) and (9) and adding gives:

$$\begin{aligned} &Im^2\left(\frac{Y}{f}\right) - 2P_1\, Im\left(\frac{Y}{f}\right) Re\left(\frac{Y}{f}\right) + P_1^2\, Re^2\left(\frac{Y}{f}\right) \\ &+ Im^2\left(\frac{X}{f}\right) - 2P_1\, Im\left(\frac{X}{f}\right) Re\left(\frac{X}{f}\right) + P_1^2\, Re^2\left(\frac{X}{f}\right) \\ &= [P_1^2 Re^2(Z) - 2P_1 Re(Z)\, Im(Z) + Im^2(Z)\,]\,(\cos^2\theta_2 + \sin^2\theta_2) \end{aligned} \tag{10}$$

where $Re^2(\quad) = [Re(\quad)]^2$ and $Im^2(\quad) = [Im(\quad)]^2$

Rearranging (10) yields the quadratic form:

$$aP_1^2 + bP_1 + C = 0 \tag{11}$$

where $a = Re^2(\frac{Y}{f}) + Re^2(\frac{X}{f}) - Re^2(Z)$

$$b = 2[Re(Z)Im(Z) - Re(\frac{Y}{f}) Im(\frac{Y}{f}) - Re(\frac{X}{f}) Im(\frac{X}{f})]$$

$$c = Im^2(\frac{Y}{f}) + Im^2(\frac{X}{f}) - Im^2(Z)$$

By an entirely similar derivation, P_2, defined by

$$P_2 = \frac{Im(Z_2)}{Re(Z_2)}$$

satisfies the same quadratic equation.

Thus, P_1 and P_2 are the two roots of the same quadratic equation.

We arbitrarily assign the two roots as

$$P_1 = \frac{-b + (b^2 - 4ac)^{1/2}}{2a}, \quad P_2 = \frac{-b - (b^2 - 4ac)^{1/2}}{2a} \tag{12}$$

Dividing (9) by (8):

$$\theta_2 = \arctan \frac{Im(\frac{X}{f}) - P_1 Re(\frac{X}{f})}{Im(\frac{Y}{f}) - P_1 Im(\frac{Y}{f})} \tag{13}$$

Similarily,

$$\theta_1 = \arctan \frac{Im(\frac{X}{f}) - P_2 Re(\frac{X}{f})}{Im(\frac{Y}{f}) - P_2 Re(\frac{Y}{f})} \tag{14}$$

If we now let

$$A_1 = |A_1| e^{j\phi_1}, \quad A_2 = |A_2| e^{j\phi_2} \tag{15}$$

then, clearly,

$$\phi_1 = \text{arc tan } P_1 \text{ and } \phi_2 = \text{arc tan } P_2.$$

Equation (3) becomes

$$Z = |A_1| e^{i\phi_1} + |A_2| e^{i\phi_2} \tag{16}$$

Multiplying (16) by $e^{-i\phi_2}$ and taking the imaginary part of the result:

$$-\text{Re}(Z)\sin\phi_2 + \text{Im}(Z)\cos\phi_2 = |A_1|\sin(\phi_1 - \phi_2)$$

and
$$|A_1| = \frac{\text{Im}(Z)\cos\phi_2 - \text{Re}(Z)\sin\phi_2}{\sin(\phi_1 - \phi_2)} \quad \text{or} \quad \frac{\text{Im}(Z) - P_2\text{Re}(Z)}{\sin\phi_1 - P_2\cos\phi_1} \tag{17}$$

Similarily

$$|A_2| = \frac{\text{Im}(Z)\cos\phi_1 - \text{Re}(Z)\sin\phi_1}{\sin(\phi_2 - \phi_1)} \quad \text{or} \quad \frac{\text{Im}(Z) - P_1\text{Re}(Z)}{\sin\phi_2 - P_1\cos\phi_2} \tag{18}$$

APPENDIX B: Derivation of the Ellipticity Filter for Mixed Rayleigh and Love Events

As in the previous derivation, the superposition equation defining the observables may be written as

$$X = -f A_1 \sin\theta_1 - B_2 \cos\theta_2 \tag{1}$$

$$Y = -f A_1 \cos\theta_1 + B_2 \sin\theta_2 \tag{2}$$

$$Z = A_1 \tag{3}$$

where A_1 is the complex amplitude of the Rayleigh event,

B_2 is the complex amplitude of the Love event,

θ_1, θ_2 are the azimuths of A_1 and B_2 respectively,

f is the apparent ellipticity.

From (1) and (2)

$$\mathrm{Re}(Y) = \mathrm{Re}(-fZ)\cos\theta_1 + \mathrm{Re}(B_2)\sin\theta_2 \tag{4}$$

$$\mathrm{Im}(Y) = \mathrm{Im}(-fZ)\cos\theta_1 + \mathrm{Im}(B_2)\sin\theta_2 \tag{5}$$

Let $P = \mathrm{Im}(-fZ)/\mathrm{Re}(-fZ)$. Multiply (4) by P:

$$P\cdot\mathrm{Re}(Y) = \mathrm{Im}(-fZ)\cos\theta_1 + P\cdot\mathrm{Re}(B_2)\sin\theta_2 \tag{6}$$

Subtracting (6) from (5):

$$\mathrm{Im}(Y) - P\cdot\mathrm{Re}(Y) = [\mathrm{Im}(B_2) - P\,\mathrm{Re}(B_2)]\sin\theta_2 \tag{7}$$

From (3)

$$\mathrm{Re}\,(X) = \mathrm{Re}\,(-fZ)\sin\theta_1 - \mathrm{Re}\,(B_2)\cos\theta_2 \tag{8}$$

$$\mathrm{Im}\,(X) = \mathrm{Im}\,(-fZ)\sin\theta_1 - \mathrm{Im}\,(B_2)\cos\theta_2 \tag{9}$$

Multiplying (8) by P and subtracting from (9):

$$\mathrm{Im}(X) - P\cdot\mathrm{Re}(X) = [P\,\mathrm{Re}\,(B_2) - \mathrm{Im}(B_2)]\cos\theta_2 \tag{10}$$

From the ratio of (7) to (10):

$$\theta_2 = -\arctan\frac{\mathrm{Im}\,(Y) - P\,\mathrm{Re}(Y)}{\mathrm{Im}\,(X) - P\,\mathrm{Re}(X)} \tag{11}$$

Rearranging (4) and (8) and taking their ratio:

$$\tan\theta_2 = -\frac{\mathrm{Re}(Y) + \mathrm{Re}(fZ)\cos\theta_1}{\mathrm{Re}(X) + \mathrm{Re}(fZ)\sin\theta_1} \tag{12}$$

or

$$\mathrm{Re}(fZ)\,[\cos\theta_1 + \tan\theta_2\sin\theta_1] = -\mathrm{Re}(X)\tan\theta_2 - \mathrm{Re}(Y) \tag{13}$$

or

$$\cos(\theta_1 - \theta_2) = -\frac{\mathrm{Re}(X)\tan\theta_2 + \mathrm{Re}(Y)}{\sec\theta_2\cdot\mathrm{Re}(fZ)} \tag{14}$$

and finally

$$\theta_1 = \theta_2 + \arccos\left[\frac{\mathrm{Re}\,(X)\sin\theta_2 + \mathrm{Re}(Y)\cos\theta_2}{\mathrm{Re}(fZ)}\right] \tag{15}$$

From (5)

$$\text{Im}\,(B_2) = \frac{\text{Im}(Y) + \text{Im}(fZ)\cos\theta_1}{\sin\theta_2} \tag{16}$$

$$\text{Re}\,(B_2) = \frac{\text{Re}(Y) + \text{Re}(fZ)\cos\theta_1}{\sin\theta_2}$$

and (1) yields A_1 as

$$\begin{aligned} \text{Re}\,(A_1) &= \text{Re}\,(Z) \\ \text{Im}\,(A_1) &= \text{Im}\,(Z) \end{aligned} \tag{17}$$

REFERENCES

1. Alexander, S.S., "Long-Period Seismic Methods for Identifying Small, Underground Nuclear Explosions," Prepared for the Air Force Office of Scientific Research under the Sponsorship of Advanced Research Projects Agency, June 1969 to March 1973.

2. Capon, J.,"Analysis of Rayleigh-Wave Multipath Propagation at LASA," Bulletin of the Seismological Society of America, Vol.60, No.5, pp. 1701-1731, October 1970.

3. Capon, J. and Everden, J.F., "Detection of Interfering Rayleigh Waves at LASA," Bulletin of the Seismological Society of America, Vol.61, No.4, pp. 817-849, August 1971.

4. Choy, G. and McCamy, K., "Enhancement of Long Period Signals by Time Varying Adaptive Filters," Lamont-Doherty Geological Observatory, unpublished.

5. Conference of the Committee of Disarmament, CCD/338, August 24, 1972.

6. Dean, W.C., "Detection Threshold of the LASA/SAAC System," Geophysical Journal of the Royal Astronomical Society, Vol.31, Nos 1-3, pp. 271-278, December 1972.

7. Savino, J.M., Murphy, A.J., Rynn, J.M.W., Tatham, R., Sykes, L.R., Choy, G.L., and McCamy, K., "Results from the High-Gain Long-Period Seismograph Experiment," Geophysical Journal of the Royal Astronomical Society, Vol.31, pp. 179-203, 1972.